

Exploring the Synergistic Anticancer Potential of Linagliptin and Esomeprazole in Cervical Cancer Cell Line: Mechanistic Insights into Targeting HSPB1, Hsp60

Aiad Gaber Arean¹, Maha Elttayef Jasim², Anas K. Awn³, Youssef Shakuri Yasin⁴, Azal Hamoodi Jumaa³

¹Al-Muthanna University/ College of Medicine / Department of medical chemistry, Iraq. ²Northern Technical University, Institute of technical Al-Dour, Department of pharmacy, Iraq. ³Iraqi National Cancer Research Center- University of Baghdad, Baghdad, Iraq. ⁴Bilad Alrafidain University, Iraq.

Abstract

Objective: This study assessed the anticancer properties of the linagliptin-esomeprazole combination and investigated its molecular mechanism by analyzing its ability to target heat shock proteins. **Methods:** Over 24 and 72 hours, a HeLa cell line was used to assess the cytotoxicity of linagliptin, esomeprazole, the linagliptin-esomeprazole mixture, and cisplatin. The safety and selective toxicity of the mixture were evaluated using the human-derived adipose tissue cell line NHF. The concentrations of linagliptin, esomeprazole, cisplatin, and the mixture ranged from 0.1 to 1000 µg/ml. The study involved an estimated combination index value to assess the potential synergistic effect of linagliptin and esomeprazole. The dose reduction index was used to evaluate decreases in the cytotoxic concentrations of the mixture components, indicating the mixture's safety and potency. The study uses computational molecular docking simulations to evaluate the binding affinity of linagliptin and esomeprazole to different cancer-related heat shock proteins. **Results:** Our study's findings show that linagliptin, esomeprazole, and their combination inhibit the growth of cervical cancer cells, with the mixture being more cytotoxic than either individual drug and cisplatin. The interaction between linagliptin and esomeprazole demonstrated synergistic cytotoxicity, as the combination index score indicated. The mixture displayed selective toxicity toward cancer cells, suggesting a lower risk of adverse effects, supported by the selective toxicity and dose reduction indexes. The pilot study of computational molecular docking simulations involving various Heat shock proteins showed optimal interactions of linagliptin and esomeprazole with HSPB1 and Hsp60, respectively, with docking scores of -8.8 kcal/mol and -7.6 kcal/mol. **Conclusion:** The findings from our study, including the MTT assay, combination index, dose reduction index, selective toxicity index, and computational docking simulations, indicate that the linagliptin-esomeprazole mixture is a promising, effective, safer, and cost-efficient alternative to traditional chemotherapy for cervical cancer.

Keywords: Linagliptin- esomeprazole- Hela cell line- heat shock protein 60- HSBB1

Asian Pac J Cancer Biol, **10 (3)**, 645-657

Submission Date: 04/22/2025

Acceptance Date: 06/14/2025

Introduction

Cervical cancer impacts 500,000 women each year, resulting in more than 300,000 fatalities. Low- and middle-income nations comprise 90% of cervical cancer incidences. In the last three decades, organized screening initiatives have decreased the incidence and mortality of cervical cancer in high-income nations by

50%. Following diagnosis, treatment options and local resources are contingent upon the severity of the illness. A radical hysterectomy, chemotherapy, or a combination of both may be required [1]. Multiple randomized clinical trials showed that women with invasive cervical cancer who are suitable for radiation treatment should choose

Corresponding Author:

Dr. Youssef Shakuri Yasin
Bilad Alrafidain University, Iraq.
Email: dryoussef@bauc14.edu.iq

cisplatin-based chemoradiotherapy [2-7]. An analysis of 18 research trials conducted across 11 countries indicates that combination chemoradiation benefits prognosis. The research demonstrated an enhancement in 12% of overall survival rates and advancements in administering both local and distant disease progression [8].

Chemoradiotherapy serves as a primary treatment for cervical cancer; nonetheless, the adverse effects associated with chemotherapy underscore the necessity for safer alternatives. Numerous trials have been conducted to determine an effective treatment for cervical cancer through the repurposing of a medication originally developed for a different therapeutic application [9-12].

Several attempts have been made to find a better and safer way to treat cancer, such as moving drugs that are already on the market for cancer therapy. Linagliptin and esomeprazole are two examples of drugs that may be able to fight cancer. The criteria for selecting these drugs were based on their comprehensive pharmacokinetic studies, safety profiles, and their demonstrated anticancer capabilities, which were supported by several studies.

Linagliptin, an antidiabetic agent, impedes the survival, growth, and motility of Glioblastoma multiforme cancer cells. Via regulates phosphorylated NF- κ B, cell cycle proteins, and cell adhesion proteins [13]. Linagliptin is believed to activate the apoptotic pathway, thereby reducing the viability of osteosarcoma cancer cells [14]. Furthermore, one of the suggested anticancer mechanisms of linagliptin occurs via targeting Hsp90 [15].

On the other hand, the anticancer properties of esomeprazole have been extensively investigated. Certain investigations associate the anticancer properties of esomeprazole with the inhibition of V-ATPase. [16] and fatty acid synthase (FASN).[17-22]. It induces apoptosis in cancer cells and enhances drug delivery by inhibiting V-ATPase and subsequent modulation of pH. V-ATPase is present in cancer cells and plays a role in regulating intra- and extracellular pH [23].

Pre-treatment of chemotherapy by omeprazole and esomeprazole enhances the response of weakly basic chemotherapeutics, such as cisplatin, 5-fluorouracil, and vinblastine, in multidrug-resistant cells [18]. Additionally, it was shown that omeprazole and lansoprazole enhanced the delivery of the weakly basic anticancer drug doxorubicin in three-dimensional breast cancer spheroids [24].

(PPIs) can notably inhibit the invasion and migration of aggressive cancer cells associated with epithelial-mesenchymal transition (EMT), a critical phase in metastasis [25, 26]. The expression alterations of E-cadherin and mesenchymal markers, including vimentin, fibronectin, and N-cadherin, represent critical characteristics of the epithelial-mesenchymal transition [27]. PPIs inhibit Snail expression, which may trigger epithelial-mesenchymal transition (EMT) without affecting the expression of other transcription factors related to EMT [12, 28-31]. PPIs demonstrated a substantial ability to bind directly to the Snail protein by disrupting CREB-binding protein (CBP)/p300-mediated Snail acetylation, thereby facilitating Snail degradation [32].

Recent studies indicate that heat shock proteins (HSPs) are often overexpressed in multiple cancer types [33-35], and they are essential in tumor cell proliferation, invasion, differentiation, metastasis, and apoptosis. The primary finding indicates that these proteins led to the overexpression of various tumors [36]. An example of these cancer-related HSBs is HSB1 (Hsp70) and Hsp60.

HSPB1, also known as Hsp27, is critical in cervical cancer. It inhibits apoptosis by interacting with essential apoptotic proteins, including caspases and BAX, while stabilizing the mitochondrial membrane. The anti-apoptotic function facilitates the survival of cancer cells in response to stressors, including chemotherapy and radiation [37]. Overexpression of HSPB1 is significantly linked to tumorigenesis, metastasis, and invasiveness, resulting in poor prognosis across various cancer types [38, 39]. The cytoprotective function of HSP27 is associated with its chaperone activities, direct modulation of the apoptosis pathway, enhancement of drug resistance, and regulation of cytoskeletal dynamics [40]. HSP27 has demonstrated the ability to safeguard cells against death signals triggered by various mechanisms, including apoptosis, necrosis, and diverse physiological stresses [37, 41]. HSP27 inhibits both intrinsic and extrinsic apoptotic pathways by binding its small or large oligomeric form to cytochrome C or death domain-associated protein (DAXX), respectively [37, 42]. HSP27 inhibits caspase 9, dependent on the activity of Bcl-2-associated X protein (BAX), which is activated by BH3 domain death agonist (BID). HSP27 interacts with protein kinase C delta type (PKC δ) and enhances resistance to cancer therapy [43]. The association between HSP27 and the inhibitor of kappa light polypeptide gene enhancer in B-cells, alpha (I κ B α), is crucial in the activation of the nuclear factor kappa-light-chain-enhancer of activated B cells (NF κ B) [44]. HSB1 interacts with the microtubule and actin proteins, which are crucial for preserving cytoskeletal integrity and may promote cell survival and invasion [45]. Consequently, because of its implicated involvement in cancer, multiple drugs have been developed to target Hsp 27, including OGX-427 (Apatorsen) [46, 47], Quercetin [48], Triptolide [49], J2 (HSP27 Inhibitor Peptide) [50].

Another crucial HSB in cancer is Hsp60. It plays an essential role in cancer development and the transport and folding of mitochondrial proteins. It is also associated with various cancer types [51]. Numerous studies indicate that HSP60 plays a role in apoptosis by promoting the activation of pro-caspase-3 through various caspases, such as caspase-6. HSP60, located in the cytosol, prevents the translocation of the pro-apoptotic protein Bax into mitochondria, thereby promoting cell survival [52].

The prognostic association of HSP60 with cervical cancer has recently emerged as a crucial area of investigation. Studies have assessed the prognostic relevance of HSP60 in cervical cancer through the application of 2-dimensional Electrophoresis (2-DE), semi-quantitative reverse transcriptase polymerase chain reaction (RT-PCR), and Western Blot (WB) analyses. The findings indicate that HSP60 is essential in the progression of cervical cancer [53]. Data from patients with advanced

prostate cancer revealed a significant correlation between HSP60 expression and tumor progression. The expression of HSP 60 shows a significant correlation with androgen independence in cases of locally advanced prostate cancer. The extent and range of HSP60 immunoreactivity functioned as indicators for biochemical recurrence in prostate cancer patients. This study indicated that patients exhibiting intense HSP60 staining in biopsy samples had shorter recurrence-free survival than those with weak HSP60 expression. A study of patients with prostate cancer demonstrated that HSP60 expression is elevated in prostate cancer tissues relative to normal prostatic tissue [54-56]. Related to the crucial role of Hsp60 in cancer, Multiple efforts were made to identify medications capable of targeting it, including mizoribine, Epolactaene, myrtilcommulone, stephacidin B, and avrainvillamide [57, 58].

Integrating currently marketed drugs for non-cancer therapeutic uses is a viable approach for formulating successful cancer therapies. Several studies have been conducted on this topic, one of which has shown that the combination of amygdalin and esomeprazole effectively eradicates cervical cancer cells. The efficacy of this combination depended on the concentration of the medicine and the duration of incubation [59, 60]. Another recent study indicated that the amalgamation of laetrile and vinblastine markedly inhibited the proliferation of esophageal cancer, revealing a synergistic interaction between the combination's constituents [61, 62]. Another study demonstrates that the combination of ciprofloxacin and laetrile efficiently inhibits the proliferation of esophageal cancer cells [63].

Although many studies have been performed on this topic, they have been limited in demonstrating the anticancer effects of the linagliptin-esomeprazole combination and its ability to target HSBB1 and Hsp60 in cancer cells. The present study was performed to address this issue.

Materials and Methods

Medications

Samarra Pharmaceutical Factory provided the study medications as raw materials. The drugs were diluted using RPMI medium (Sigma-Aldrich (Merck)-Germany) to obtain concentrations varying from 0.1 µg/ml to 1000 µg/ml.

Cytotoxic assay

First, the cancer cell line (HeLa cell line), sourced from a human malignant cervical cancer, and the Normal human-derived adipose tissue (NHF) cell line were maintained and grown at the tissue culture section of ICCMGR. The cells were seeded in 75 cm² tissue culture flasks under regulated conditions, sustaining a relative humidity of 37°C and 5% CO₂. The cells were grown in 10% fetal bovine serum RPMI-1640 media (Sigma Chemicals, England) supplemented with 100 U/mL of penicillin-streptomycin (100 µg/mL streptomycin) [64, 59].

Using a 96-well microtiter plate to grow cervical cancer cells and human adipose tissue cells, the cytotoxicity of each linagliptin, esomeprazole, cisplatin, and the mixture was evaluated. The cancer cells' proliferation elevation was steady and progressive throughout the logarithmic growth phase. The cytotoxicity of study medications was tested over two distinct incubation periods: 24 hours and 72 hours [65].

Each well in a 96-well microtiter plate contains about 10,000 cells. A medium containing 10% fetal bovine serum is required to grow the cells. The plates were incubated at 37°C for 24 hours to promote cell adhesion. The RPMI medium was prepared without serum and used for serial dilutions. In RPMI medium that did not include calf serum, linagliptin, esomeprazole, and their mixture were diluted. A range of dilutions was made for every drug, starting at 0.1 and increasing to 1000 µg/ml [63, 66].

After 24 hours of cancer cell growth, each concentration of diverse study treatments was distributed to six wells, and the same number was applied to control groups. Each well received 200 µl of RPMI medium containing the treatments. Control wells received 200 microlitres of maintenance media, with exposure times ranging from one to three days. The plates were placed back into the incubator with a firm attachment with the self-adhesive substance. The cells were subsequently treated with MTT dye.

The optical density of each well was measured using a microtiter plate reader (ELISA reader) operating at a transmission wavelength of 550 nm [67, 68].

The following mathematical equation is employed to estimate the growth inhibition rate: [68]

Growth inhibition % = (optical density of control wells - optical density of treated wells) / (optical density of control wells) * 100%

Selective toxicity index

This test was employed to estimate the mixture and cisplatin's selective toxicity toward cancer cells at each incubation period (24 and 72 hours). The selective cytotoxicity index was determined using the following formula after calculating the IC₅₀ level for the mixture and cisplatin by employing a cell proliferation curve for each of the two cell lines, HeLa and NHF cell lines [69].

Selective toxicity Index (SI) = (IC₅₀ of normal cell lines) / (IC₅₀ of cancer cell lines) × 100

An SI score greater than 1.0 suggests that a drug exhibits superior efficacy in targeting tumor cells compared to its toxicity toward normal cells.

Molecular docking

Linagliptin and esomeprazole's chemical structures were meticulously generated utilizing ChemDraw software (Cambridge Soft, USA) and subsequently refined through Chem3D. Depending on the outcomes of a pilot study into the chemical docking of linagliptin and esomeprazole with various cancer-associated heat shock proteins, HSPB1 (heat shock protein beta1 or Hsp27)

and Hsp60 (heat shock protein 60 chaperonins) were selected. The molecular structure of HSPB1 (PDB: 3q9q) and Hsp60 (PDB: 4pj1) was acquired from the Protein Data Bank.

Utilizing AutoDock Tools, optimization and modification of protein structures were achieved. AutoDock Tools determined the most favorable conformation of the ligands, creating a PDBQT file for the ligands.

After optimization, the ligands (linagliptin and esomeprazole) structures and the human HSPB1 and Hsp60 chaperone proteins were input into AutoDock-Tools. The docking procedure was subsequently executed utilizing the same program. The docking energy scores and binding interactions were analyzed using BIOVIA Discovery Studio, UCSF Chimera, and AutoDock Vina. [70, 71].

Drug combinations pattern assessment

(Compusyn) A computational simulator determined the scores of the combination index (CI) and dose reduction index (DRI). The CI score estimate aimed to evaluate the potential for synergistic, additive, or antagonistic interactions among the mixture's components. Concentration-effect curves can show the proportion of cells with reduced growth relative to drug concentration, measured at 24 and 72 hours of treatment. A CI score below one indicates a synergistic interaction between the drugs; a score exactly at one suggests an additive effect; and a score above one indicates an antagonistic interaction.

The DRI score estimation quantifies the degree to which the concentration of individual components in a mixture can be reduced while maintaining comparable efficacy to each drug. A DRI greater than 1 indicates a favourable concentration reduction, whereas a DRI less than 1 indicates an unfavorable dosage decrease.

Compusyn software (Biosoft, Ferguson, MO, USA) calculated the combination and dose reduction index values [72, 73].

Ethical approval

This study does not encompass human subjects within its parameters.

Statistical Analysis

The cytotoxicity assay results are expressed as mean \pm standard deviation (SD). A one-way analysis of variance (ANOVA) was employed to identify the variance among study groups. The Tukey and LSD tests were utilized to examine the distinctions among various groups. The research employed the statistical software SPSS version 20, establishing a significance threshold at $p < 0.05$ [74].

Results

Cytotoxicity assay

We initially assessed the cytotoxicity of each component before evaluating the cytotoxic effects of the linagliptin-esomeprazole mixture. This preliminary assessment sought to elucidate cytotoxicity mechanisms and examine the interactions between the mixture's components, specifically assessing whether these interactions demonstrate synergistic, antagonistic, or additive effects.

Linagliptin Cytotoxicity

The study found that linagliptin's cytotoxicity demonstrated its ability to suppress the proliferation of cervical cancer cells in a concentration- and time-dependent manner, with a decrease in the IC_{50} level observed from 24 to 72 hours. Supported time-dependent pattern of cytotoxicity Table 1.

Esomeprazole cytotoxicity

The MTT assessments demonstrated that the antiproliferative properties of esomeprazole varied significantly with changes in drug concentrations and time incubation Table 1.

Cisplatin cytotoxicity

The study explored cisplatin cytotoxicity to serve as a positive control for comparative purposes. The established time and concentration factors influence cisplatin cytotoxicity in both HeLa and HNF cell lines. With a relatively similar cytotoxic impact in each cell line Table 2.

(linagliptin -esomeprazole) mixture cytotoxicity

Table 1. The Effect of Esomeprazole, Linagliptin on Cervical Cancer Viability at 24 and 72 hours

Concentration (µg/ml)	Inhibition of cellular proliferation (mean ± SD ^a)					P- value
	Esomeprazole			Linagliptin		
	24 hrs.	72 hrs.	P- value	24 hrs.	72 hrs.	
0.1	C 0.00 ±0.000	D 2.00± 1.000	0.026*	C 2.00 ± 1.000	C 14.00 ± 4.000	0.007*
1	C 1.00± 1.000	CD 8.00± 3.000	0.019*	C 7.00 ± 2.000	BC 25.00 ± 5.000	0.001*
10	C 5.00± 1.000	BC 13.00± 3.000	0.012*	B 16.00 ± 4.000	B 30.00 ± 2.000	0.008*
100	B 17.00±2.000	B 21.00± 1.000	0.036*	AB 22.00 ± 2.000	AB 33.00 ± 4.000	0.006*
1000	A 35.00± 2.000	A 39.00± 4.000	0.196	A 29.00 ± 1.000	A 40.00 ± 1.000	0.004*
^b LSD value	5.14	9.76	-	8.3	11.74	-
IC ₅₀	1448.8 µg/ml	1339 µg/ml	-	2072.2 µg/ml	1589.5 µg/ml	-

a, standard deviation; b, least significant difference; statistically significant differences are shown by variations in capital letters within the same column; *, significant at ($P < 0.05$)

Table 2. Cisplatin Impact on HeLa and NHF Cell Line Proliferation at 24 and 72 hours

Concentration ($\mu\text{g/ml}$)	Inhibition of cellular proliferation (mean \pm SD ^a)					
	HeLa cell line			NHF cell line		
	24 hrs.	72 hrs.	P- value	24 hrs.	72 hrs.	P- value
0.1	D 0.00 \pm 0.000	D 2.00 \pm 1.000	0.026*	D 0.00 \pm 0.000	C 8.00 \pm 4.000	0.026*
1	D 2.00 \pm 2.000	D 7.00 \pm 2.000	0.038*	CD 3.00 \pm 3.000	C 15.00 \pm 5.000	0.023*
10	C 10.00 \pm 3.000	C 20.00 \pm 2.000	0.009*	C 11.00 \pm 3.000	B 33.00 \pm 3.000	0.001*
100	B 29.00 \pm 2.000	B 38.00 \pm 1.000	0.002*	B 31.00 \pm 1.000	B 47.00 \pm 3.000	0.001*
1000	A 37.00 \pm 2.000	A 58.00 \pm 3.000	0.001*	A 40.00 \pm 3.000	A 60.00 \pm 4.000	0.002*
^b LSD value	7.46	7.1	-	8.62	14.1	-
IC ₅₀	1380.5 $\mu\text{g/ml}$	778.8 $\mu\text{g/ml}$	-	1256.5 $\mu\text{g/ml}$	682.3 $\mu\text{g/ml}$	-

a, standard deviation; b, least significant difference; Capital letter variations within the same column signify statistically significant differences. *, significant at ($P < 0.05$)

Study findings demonstrated the ability of the mixture to inhibit cervical cancer cell growth in each incubation period, reaching up to 51 and 68 growth inhibition percentages for each 24 and 72-hour incubation, respectively. These findings and the IC₅₀ level supported the time-dependent manner of mixture cytotoxicity. Furthermore, variation in mixture concentrations causes variation in its cytotoxicity, reflecting a concentration-dependent manner of cytotoxicity Table 3.

In contrast, the mixture had a less cytotoxic effect on the NHF cell line than on the HeLa cell line. The comparison of the mixture's cytotoxicity on HeLa and NHF cell lines revealed significant differences in cytotoxic effects across all concentrations and incubation periods. Table 4.

A further comparison across all treatment options revealed the mixture's cytotoxicity superiority over its components and cisplatin, especially after 27 hours of incubation Figure 1.

Selective toxicity index assessment

The selective toxicity index score for the linagliptin–esomeprazole combination was 7.83 at 24 hours and 11.61 at 72 hours, indicating that the combination exhibits selective toxicity toward cancer cells compared to normal healthy cells, with an increase in the selectivity index

associated with longer incubation periods. In contrast, cisplatin's selective toxicity index score was 0.91 at 24 hours and 0.54 at 72 hours, indicating an unevaluable selective toxicity toward cancer cells compared to normal healthy cells Figure 2.

Molecular docking studies

A computational molecular docking simulation was employed to assess the affinity of each linagliptin and esomeprazole for binding with a diver's array of cancer-related heat-shocked proteins. The outcomes exhibited that the best interaction of linagliptin was found with (PDB code: 3q9q), with a docking score equal to (-7.6) kcal/mol. Meanwhile, esomeprazole had a higher affinity for binding with Hsp 60 (PDB code: 4pj1) with a docking score equal to (-8.8) kcal/mol. The study utilized AutoDock tools version 1.5.7, BIOVIA Discovery Studio UCSF Chimera, and AutoDock Vina [75].

Molecular docking analysis for binding linagliptin with HSPB1 was presented. Subsequently, two conventional hydrogen bonds formed with the HIS A:103 and ARG A:136 amino acid residues at 1.85 Å and 2.94 Å distances. One carbon-hydrogen bond formed with the ARG A:136 amino acid residues at a 3.53 Å distance. One pi-cation bond formed with the ARG A:140 amino acid residues at a 4.56 Å distance. Two pi-pi-stacked bonds formed with

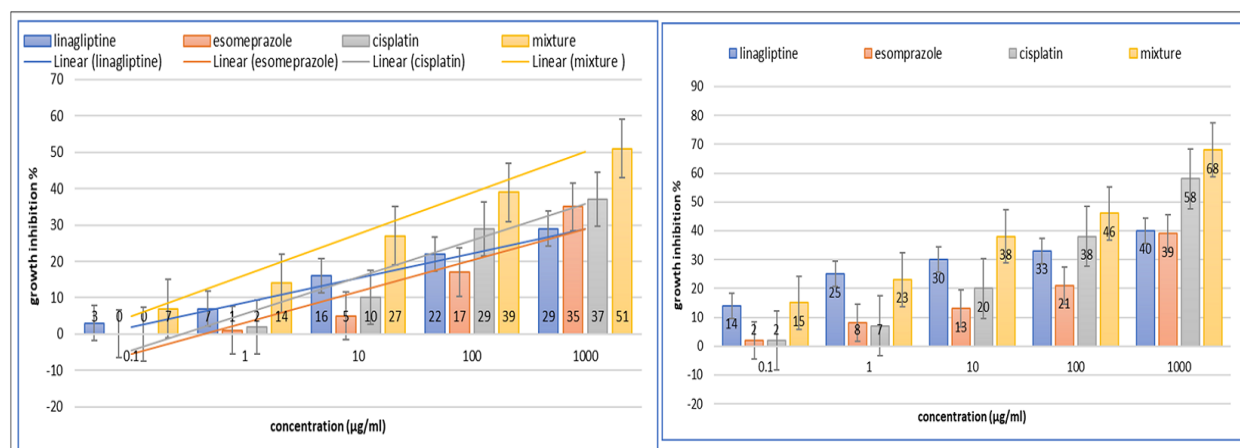


Figure 1. A Comparison of Growth Inhibition by Linagliptin, Esomeprazole, Cisplatin, and a Mixture. Error bars, SE. 24-hour incubation (right), 72-hour incubation (left)

Table 3. Mixture Impact on HeLa and NHF Cell Line Proliferation at 24 and 72 Hours

Concentration (µg/ml)	Inhibition of cellular proliferation (mean ± SD ^a)					
	HeLa cell line			NHF cell line		
	24 hrs.	72 hrs.	P- value	24 hrs.	72 hrs.	P- value
0.1	D 7.00±2.000	D 15.00±5.000	0.062	B 0.00 ±0 .000	B 1.00±1.000	0.158
1	D 14.00±4.000	CD 23.00±3.000	0.036*	B 1.00 ±1.000	B 3.00±2.000	0.196
10	C 27.00±5.000	BC 34.67±7.572	0.217	AB 2.00±1.000	AB 5.00±1.000	0.021
100	B 39.00±2.000	B 46.00±1.000	0.006*	AB 4.00±2.000	AB 6.00±3.000	0.391
1000	A 51.00±1.000	A 68.00±2.000	0.0001*	A 8.00±3.000	A 11.00±1.000	0.176
^b LSD value	11.5	15.98	-	6.3	6.5	-
IC ₅₀	923 µg/ml	520.2 µg/ml	-	7236 µg/ml	6040.4 µg/ml	-

a, standard deviation; b, least significant difference. Capital letter variations within the same column signify statistically significant differences. *, significant at (P<0.05)

two PHE A:138 amino acid residues at 4.77 Å and 5.27 Å of distance. One alkyl bond formed with the ARG A:136 amino acid residues at 4.75 Å of distance. Two pi-alkyl bond formed with LEU A:99 and ARG A:140 amino acid residues at 5.10 Å and 5.02 Å of distance, subsequently. Figure [3].

For comparative purposes, J2, a HSPB1 inhibitor [50], was studied, yielding a docking score of (-5.7) kcal/mol. A molecular docking study regarding J2 binding to HSPB1 was presented. One conventional hydrogen bond formed with PHE A:104 amino acid residues at 2.81 Å. One pi-sigma bond formed with PHE A:138 amino acid residues at 3.92 Å. Two pi-pi-T-shaped bonds formed with two PHE A:104 amino acid residues at 5.41 Å and 4.86 Å of distance. Finally, three alkyl bonds formed with ARG A:136, LEU A:99, and ARG A:140 amino acid residues at 4.44 Å, 4.24 Å, and 4.74 Å of distance Figure 3.

While Molecular docking analysis for binding esomeprazole with Hsp60 presented, three conventional hydrogens bound formed with two LYS A:51 and one ILE A:150 amino acid residues at 2.31 Å, 2.68 Å, and 2.41 Å of distance subsequently. One carbon-hydrogen bond formed with the ASP A:399 amino acid residues at 3.71 Å distance. one pi-anion hydrogen bond formed with the ASP A:87 amino acid residues at 3.77 Å distance. One pi-sigma hydrogen bond formed with the ILE A:150 amino acid residues at 3.95 Å distance. Two alkyl bonds formed with ILE A:150 and ILE A:494 amino acid residues at 4.78 Å and 4.98 Å of distance, subsequently. Eventually, four pi-alkyl bound formed with two PRO A:33, ILE A:150, and ILE A:494 amino acid residues at a 4.91 Å, 3.93 Å, 4.13 Å, and 5.27 Å distance, subsequently Figure 3.

For comparative purposes, mizoribine, a Hsp60 inhibitor [76], was studied, yielding a docking score of (-7.9) kcal/mol. A molecular docking study regarding mizoribine binding to Hsp90 was presented. Nine conventional hydrogens bound formed with GLY A:53, GLY A:88, two THR A:89, two THR A:91, ASP A:52, and ASP A:399 amino acid residues at 2.02 Å, 2.79 Å, 2.52 Å, 2.66 Å, 2.76 Å, 2.53 Å, 2.73 Å, 2.02 Å, and 2.75 Å of distance. Subsequently, two carbon-hydrogen bonds formed with ASP A:52 and GLY A:88 amino acid residues at 3.28 and 3.45 Å distances. Finally, one pi-anion bond formed with the ASP A:87 amino acid residues at 4.12.

Figure 3.

Identifying the Maximizing Efficacy

Study findings to identify the potential synergistic impact between a mixture of ingredients demonstrated the subsequent results. After 24-hour incubation, the pattern of the combination of linagliptin and esomeprazole showed a Very Strong Synergism at 0.01, 0.1, and 1 µg/ml concentrations. Subsequently, 10 and 100 µg/ml concentrations showed a Strong Synergism and Nearly Additive Table 5, Figure 4.

After 72-hour incubation, the pattern of the combination of linagliptin and esomeprazole showed a Very Strong Synergism at 1, 10, and 100 µg/ml concentrations of each one. Subsequently, 0.01 and 0.1 µg/ml concentrations showed slight antagonism and strong synergism. Table 5, Figure 4.

The dose reduction index outcomes indicated that the drugs in the mixture required to induce cytotoxicity decreased compared to their concentrations when used individually. This reduction was observed at all time intervals (24 and 72 hours of incubation) for all concentrations of linagliptin and esomeprazole, except for the lowest concentration of linagliptin, indicating a favorable decrease in the effective cytotoxic concentration of the combination components, suggesting less likelihood of mixture drug adverse effects. Table (5)

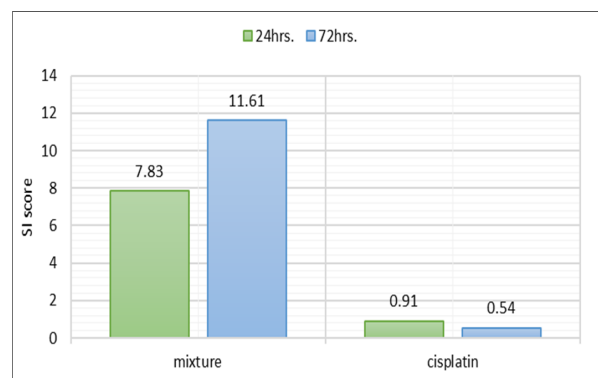


Figure 2. The Selective Toxicity Index of Linagliptin-Esomeprazole Mixtures and Cisplatin Across 24 hours. And 72 hours. Incubation period. (An SI greater than 1.0 signifies a drug's enhanced efficacy against tumor cells compared to its toxicity toward normal cells.

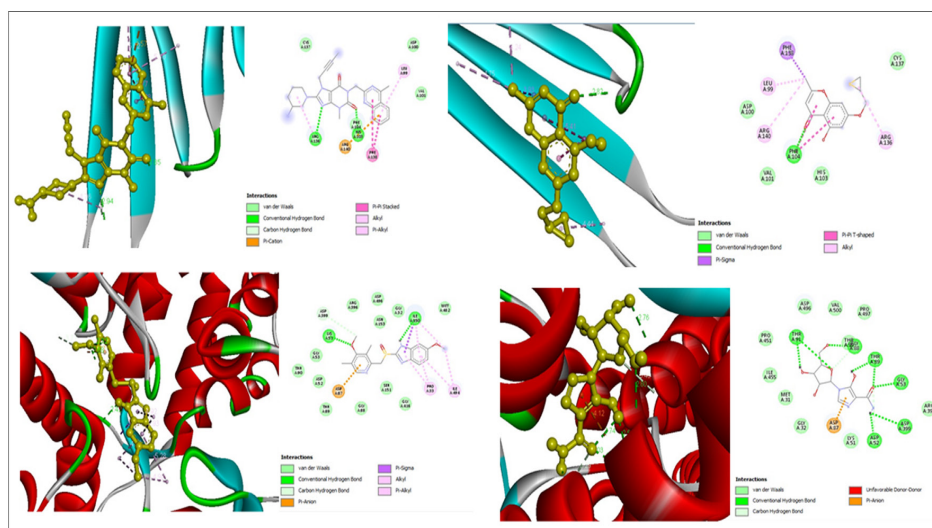


Figure 3. 2D and 3D Structure of Human Hspβ1 (above) Binding Site with Linagliptin (right above), J2 (left above). And Hsp60 (below) Binding Site with Esomeprazole (right below), Mizoribine (left below)

Table 4. A Comparison of the Mixture Impact on HeLa and NHF Cell Line Proliferation at 24 and 72 hours

Concentration (μg/ml)	Inhibition of cellular proliferation (mean ± SD ^a)					
	HeLa cell line			NHF cell line		
	24 hrs.	72 hrs.	P- value	24 hrs.	72 hrs.	P- value
0.1	D 7.00±2.000	D 15.00±5.000	0.062	B 0.00 ±0 .000	B 1.00±1.000	0.158
1	D 14.00±4.000	CD 23.00±3.000	0.036*	B 1.00 ±1.000	B 3.00±2.000	0.196
10	C 27.00±5.000	BC 34.67±7.572	0.217	AB 2.00±1.000	AB 5.00±1.000	0.021
100	B 39.00±2.000	B 46.00±1.000	0.006*	AB 4.00±2.000	AB 6.00±3.000	0.391
1000	A 51.00±1.000	A 68.00±2.000	0.0001*	A 8.00±3.000	A 11.00±1.000	0.176
^b LSD value	11.5	15.98	-	6.3	6.5	-
IC ₅₀	923 μg/ml	520.2 μg/ml	-	7236 μg/ml	6040.4 μg/ml	-

a, standard deviation; b, least significant difference. Capital letter variations within the same column signify statistically significant differences. *, significant at (P<0.05)

Figure (4).

The CI (Combination Index) and DRI (Dose Reduction Index) Values were evaluated utilizing Compusyn software. A CI score below one indicates a synergistic interaction between the drugs; a score exactly at one suggests an additive effect; and a score above one indicates an antagonistic interaction. A dose reduction index (DRI) exceeding one correlates with reduced toxicity [77].

Histopathological features of the study cell lines

Figure 5 shows the morphological changes in the HeLa and NHF cell lines after 72 hours of treatment.

Discussion

The study aimed to find an effective and safe anticancer treatment. This aim may be attained via many ways that diverge from conventional anticancer therapies. A diverse array of drugs used for many illness situations, apart from cancer, may exhibit anticancer properties. In conjunction with this concept, we study the anticancer effects of the combination of linagliptin (an antidiabetic) and esomeprazole (an antacid). The selection of these medications is based on findings from multiple

prior studies suggesting the anti-cancer properties of each medication. Additionally, each medication was meticulously inspected regarding its pharmacokinetics and safety profile.

Study outcomes of the MTT assay, combination index, and selectivity index demonstrated that each linagliptin and esomeprazole exhibited a harmful impact on cervical cancer while showing less cytotoxicity toward normal cells. At the same time, mixing them exhibited superior anticancer properties over the cisplatin cytotoxicity and each mixture ingredient alone via a synergism effect between the mixture ingredients. Furthermore, from a safety perspective and concerning the dose reduction index, the findings indicate that the mixture has a lower probability of adverse effects than its components. The mixture's safety is further supported by its favorable selectivity index score, indicating its role as a targeted treatment for cancer.

The histopathological analysis of HeLa cell line slides substantiates the results obtained from the MTT assay, exhibiting characteristic morphological changes across various treatment groups. The untreated control slide retained typical features of cervical carcinoma cells, including densely aggregated, irregular nuclei and

Table 5. Combination Index and Dose Reduction Index Value for the Cytotoxicity of Linagliptin-esomeprazole Mixture at 24 and 72 hrs. Incubation Periods

At 24 24-hour incubation period							
Concentration $\mu\text{g/ml}$		Con. ratio		CI value	Combination behaviour	DRI value	
linagliptin	ciprofloxacin	Mix	1:01			linagliptin	ciprofloxacin
0.05	0.05	0.1		0.04476	Very Strong Synergism	22.8877*	938.362 *
0.5	0.5	1		0.03342	Very Strong Synergism	35.4473*	192.067 *
5	5	10		0.03342	Very Strong Synergism	37.3030*	35.5356 *
50	50	100		0.16806	Strong Synergism	45.6942*	6.84098 *
500	500	1000		0.9685	Nearly Additive	25.7994*	1.07557 *
At 72 72-hour incubation period							
0.05	0.05	0.1	1:01	1.14936	Slight Antagonism	0.87181	430.875*
0.5	0.5	1		0.29445	Strong Synergism	3.45614*	195.742*
5	5	10		0.02547	Very Strong Synergism	52.6309*	154.674*
50	50	100		0.0441	Very Strong Synergism	52.5933 *	39.8650*
500	500	1000		0.00416	Very Strong Synergism	112527*	240.808*

increased mitotic figures. In contrast, cells subjected to the mixture displayed significant antiproliferative effects, evidenced by cellular shrinkage, nuclear pyknosis, reduced mitotic activity, cytoplasmic vacuolization, and apoptotic bodies.

To explore the anticancer mechanism of the mixture, it is necessary to explore the suggested anticancer mechanism of each mixture ingredient, which multiple previous studies have already described. Several studies have been conducted on the same issue as our study's findings regarding linagliptin. Linagliptin demonstrated a significant capacity to reduce the viability of Saos-2 cells, a human bone cancer cell line, and hFOB1.19 cells, a human fetal bone cell line [14]. Linagliptin has been shown to inhibit the survival, growth, and movement of Glioblastoma cancer cells; the pattern of growth inhibition was primarily influenced by the incubation

duration, indicating a greater dependence on time than concentration. This finding suggests that linagliptin's anticancer properties are linked to its effects on specific cell cycle stages [78].

Numerous studies have shown various anticancer mechanisms of linagliptin. Linagliptin has been shown to induce cell cycle arrest in the G2/M phase at low doses and both the G2/M and S phases at high concentrations. [78] Another proposed mechanism is that linagliptin strongly interacts with Cyclin-Dependent Kinase 1 (CDK1), an essential protein in cell cycle control. CDK1 phosphorylates many substrate proteins, including histones H1, laminin, and Rbis. Furthermore, Linagliptin demonstrates a significant inhibitory effect on cell proliferation and tumor growth through the selective targeting of Aurora kinase B and CDK1, resulting in diminished phosphorylation of Rb and a reduction

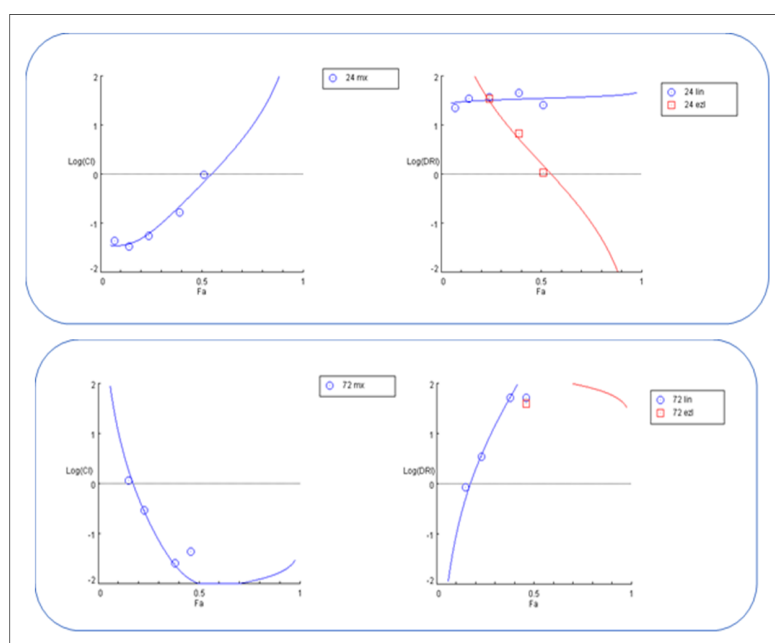


Figure 4. Log Combination Index Plot (left); dose reduction index plot (right) for the mixture at 24 hrs.(above), 72 hrs. (below), lin; linagliptin, ezl; esomeprazole, CI: combination index, DRI: dose reduction index

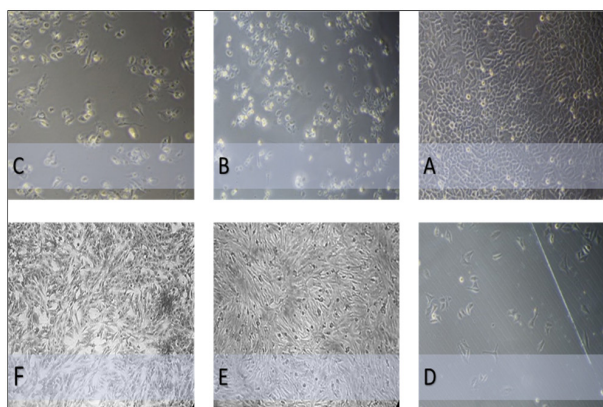


Figure 5. Morphological Features of Study Cell Lines Observed under a Phase Contrast Microscope (400X). (A) Human cervical cancer cells (HeLa cell line) were left without treatment and considered a control group. (B) Cervical cancer cells were exposed to 1000 µg/ml of esomeprazole for 72 hours. (C) Cervical cancer cells were exposed to 1000 µg/ml of linagliptin concentration for 72 hours. (D) Cervical cancer cells were subjected to a 1000 µg/ml concentration of a combination of linagliptin–esomeprazole mixture for 72 hours. (E) NHF normal cells were subjected to a 1000 µg/ml concentration of a combination of linagliptin–esomeprazole mixture for 72 hours. (F) Human-derived adipose tissue (normal cell line) was left untreated and considered a control group.

in Bcl-2 production. Pro-caspase 3 is a protein [79]. Also, Linagliptin demonstrated the ability to target Aurora kinase B selectively. This kinase is a conserved serine-threonine protein kinase within the Aurora family, essential for regulating cell division [80].

In contrast, several studies were performed to assess esomeprazole's anticancer properties. Conducting esomeprazole can inhibit the proliferation of gastric cancer cells and significantly improve their chemosensitivity, as evidenced by MTT assays. Flow cytometry analysis indicated that esomeprazole induced apoptosis and resulted in cell cycle arrest during the S and G2/M phases. [81]. A subsequent study demonstrated that proton pump inhibitors, specifically esomeprazole, may significantly impede the invasion and migration of aggressive cancer cells linked to epithelial-mesenchymal transition (EMT), an essential stage in metastasis [25, 26, 31]. E-cadherin, vimentin, fibronectin, and N-cadherin expression significantly change during the epithelial-mesenchymal transition [27]. Esomeprazole was found to inhibit Snail expression, which can induce epithelial-mesenchymal transition (EMT), while not influencing the expression of other transcription factors associated with EMT [12, 28-30]. Furthermore, Esomeprazole exhibited a significant capacity to bind directly to the Snail protein by inhibiting CREB-binding protein (CBP)/p300-mediated Snail acetylation, which promotes Snail degradation [32].

Furthermore, other Proposed mechanisms include esomeprazole's ability to induce lysosomal membrane permeabilization, leading to increased lysosomal outflow into the cytoplasm, lysis of cellular components, and subsequent cell death. Lysosomal enzymes demonstrate hydrolytic activity and establish an acidic environment that aids in eliminating tumor cells [60, 82, 83].

In addition to the anticancer mechanisms prespecified above, the current study identified novel anticancer mechanisms for linagliptin and esomeprazole, as demonstrated by the results of the molecular docking analysis, indicating their capacity to target Hsp60 and HSPB1. Each type of HSP plays a crucial role in cancer.

Hsp 60 plays an essential role in the transport and folding of mitochondrial proteins and has been reported to be associated with various cancer types [51]. Its plays a pro-apoptotic role by promoting the activation of pro-caspase-3 through various caspases, such as caspase-6. HSP60, located in the cytosol, inhibits the translocation of the pro-apoptotic protein Bax into mitochondria, thereby promoting cell survival [52].

Recently, the prognostic association of HSP60 with cervical cancer has emerged as a significant area of investigation. In these studies, the predictive value of HSP60 in cervical cancer was assessed through 2-dimensional Electrophoresis (2-DE), semi-quantitative reverse transcriptase polymerase chain reaction (RT-PCR), and Western Blot (WB) analyses. The findings strongly indicate that HSP60 is integral to the progression of cervical cancer [53].

On the other hand, HSPB1, or Hsp27, plays a crucial role in cancer. It inhibits apoptosis by interacting with key apoptotic proteins, such as caspases and BAX, and stabilizing the mitochondrial membrane. In cervical cancer, this anti-apoptotic function helps cancer cells survive under stress conditions, such as chemotherapy or radiation [37]. HSPB1 overexpression is significantly associated with tumorigenesis, metastasis, and invasiveness, leading to unfavorable prognosis in multiple cancer types [38, 39]. The cytoprotective role of HSP27 is linked to its chaperone activities, direct modulation of the apoptosis pathway, enhancement of drug resistance, and regulation of cytoskeletal dynamics [40]. HSP27 has been shown to protect cells from death signals induced in different ways, including apoptosis, necrosis, and various physiological stresses [37, 41]. HSP27 inhibits intrinsic and extrinsic apoptotic pathways by binding its small or large oligomeric form to cytochrome C or death domain-associated protein (DAXX), respectively [37, 42]. HSP27 inhibits caspase 9, contingent upon the activity of Bcl-2-associated X protein (BAX), which is activated by BH3 domain death agonist (BID). HSP27 interacts with protein kinase C delta type (PKC δ) and promotes resistance to cancer therapy [43]. The interaction between HSP27 and the nuclear factor of kappa light polypeptide gene enhancer in B-cells inhibitor, alpha (I κ B α), plays a role in the activation of the nuclear factor kappa-light-chain-enhancer of activated B cells (NF κ B) [44]. It interacts with the microtubule and actin protein, essential for maintaining cytoskeleton integrity, and may facilitate cell survival and invasion [45].

Each HSP type's valuable role in cancer positions them as a potential target for promising cancer therapies. Several studies were performed to target these cancer-related heat shock proteins, and several agents were designed for Hsp60 targeting. Such as mizoribine, Epolactaene, myrtucommulone, stephacidin B, and avrainvillamide [57, 58]. On the other side, several agents were designed

to target HSPB1, including OGX-427 (Apatorsen) [46, 47], Quercetin [48], Triptolide [49], J2 (HSP27 Inhibitor Peptide) [50].

The molecular docking study findings indicate that the linagliptin-esomeprazole mixture possesses a dual mechanism of action that involves targeting cancer cells via HSPB1 and Hsp60. This mechanism elucidates the synergistic interaction among the mixture's components. Regarding fundal consideration, the study's limitation included a lack of further laboratory investigations, including cell cycle arrest and apoptosis tests.

In conclusion, the findings of our study indicate that linagliptin, esomeprazole, and their combination inhibit the proliferation of cervical cancer cells. The combination index score demonstrates the mixture's superior cytotoxicity compared to its components and cisplatin. The interaction of linagliptin and esomeprazole exhibited synergistic cytotoxicity, as evidenced by the combination index score. The mixture demonstrated selectivity for cancer cells and a reduced probability of adverse effects, as evidenced by the selective toxicity and dose reduction indexes.

The study proposes a novel anticancer mechanism for the mixture, illustrated by computational docking simulations via its ability to target HSPB and Hsp60 with each linagliptin and esomeprazole. The variation in targeting HSB elucidates the synergistic impact between linagliptin and esomeprazole in the mixture.

The study outcomes, alongside the established pharmacokinetic, toxicological, and safety profiles of each drug mixture, indicate that the linagliptin—esomeprazole mixture represents a promising, effective, and safer anticancer option, especially for cervical cancer.

Author Contributions

Design and development: Azal Hamoody, Aiad Gaber Arian, Maha Lateef Jassim.

Gathering and organizing data: Azal Hamoody, Anas K. Awn., Youssef Shakuri.

Data analysis/interpretation: Maha Lateef Jassim, Aiad Gaber Arian, Youssef Shakuri.

Article composition: Anas K. Awn., Aiad Gaber Arian, Maha Lateef Jassim.

Critique the essay for significant ideas: Azal Hamoody, Youssef Shakuri. Maha Lateef Jassim.

Statistical analysis expertise: Aiad Gaber Arian, Maha Lateef Jassim, Anas K. Awn.

Ultimate article endorsement and guarantee: Youssef Shakuri, Azal Hamoody.

Acknowledgements

The research team acknowledges the contributions of the researchers and instructional staff at ICMGR / Mustansiriyah University in Baghdad and the Iraqi National Cancer Research Center/University of Baghdad for their essential support during the study. I want to express my gratitude to the quality control department of the Samarra Pharmaceutical Factory for providing the medication utilized in the present study.

Financial support and sponsorship

Self-funded

Conflicts of interest

The authors assert the absence of any conflict of interest.

Declaration of Generative AI and AI-assisted technologies in the writing process:

The authors state that this work does not utilize generative AI or AI-assisted technologies.

Abbreviations

(ICCMGR)The Iraqi Centre for Cancer and Medical Genetics Research.

MTT: 3-(4,5-dimethylthiazol-2-yl)-2,5-diphenyltetrazolium bromide stain

RPMI: Roswell Park Memorial Institute medium

SAS: Statistical Analysis System

LSD: Least Significant Difference

DRI: dose reduction index

CI: combination index

Hsp 60: heat shock protein 60

NHF cell line: human-derived adipose tissue cell line

PPIs: proton pump inhibitors

HSB: heat shock protein

HSB1: heat shock protein beta 1

References

1. Cohen PA, Jhingran A, Oaknin A, Denny L. Cervical cancer. *Lancet* (London, England). 2019 01 12;393(10167):169-182. [https://doi.org/10.1016/S0140-6736\(18\)32470-X](https://doi.org/10.1016/S0140-6736(18)32470-X)
2. Whitney CW, Sause W, Bundy BN, Malfetano JH, Hannigan EV, Fowler WC, Clarke-Pearson DL, Liao SY. Randomized comparison of fluorouracil plus cisplatin versus hydroxyurea as an adjunct to radiation therapy in stage IIB-IVA carcinoma of the cervix with negative para-aortic lymph nodes: a Gynecologic Oncology Group and Southwest Oncology Group study. *Journal of Clinical Oncology: Official Journal of the American Society of Clinical Oncology*. 1999 05;17(5):1339-1348. <https://doi.org/10.1200/JCO.1999.17.5.1339>
3. Eifel P, et al. Pelvic radiation with concurrent chemotherapy versus pelvic and para-aortic radiation for high-risk cervical cancer: an update of RTOG 90-01. 2002;54(2):p. 1.
4. PETERS, W.I.J.J.C.O., Cisplatin and 5-fluorouracil plus radiation therapy are superior to radiation therapy as adjunctive in high-risk early stage carcinoma of the cervix after radical hysterectomy and pelvic lymphadenectomy: report of a phase III intergroup study. 2000;18:p. 1606-1613.
5. Rose PG, Bundy BN, Watkins EB, Thigpen JT, Deppe G, Maiman MA, Clarke-Pearson DL, Insalaco S. Concurrent cisplatin-based radiotherapy and chemotherapy for locally advanced cervical cancer. *The New England Journal of Medicine*. 1999 04 15;340(15):1144-1153. <https://doi.org/10.1056/NEJM199904153401502>
6. Keys HM, Bundy BN, Stehman FB, Muderspach LI, Chafe WE, Suggs CL, Walker JL, Gersell D. Cisplatin, radiation, and adjuvant hysterectomy compared with radiation and adjuvant hysterectomy for bulky stage IB cervical carcinoma. *The New England Journal of Medicine*. 1999 04 15;340(15):1154-1161. <https://doi.org/10.1056/NEJM199904153401503>

7. Health, U.D.o. and N.I.o.H. Human Services %J Public Health Service, Bethesda, MD, NCI clinical announcement. 1999;.
8. Green JA, Kirwan JM, Tierney JF, Symonds P, Fresco L, Collingwood M, Williams CJ. Survival and recurrence after concomitant chemotherapy and radiotherapy for cancer of the uterine cervix: a systematic review and meta-analysis. *Lancet* (London, England). 2001 09 08;358(9284):781-786. [https://doi.org/10.1016/S0140-6736\(01\)05965-7](https://doi.org/10.1016/S0140-6736(01)05965-7)
9. Lapresa M, Parma G, Portuesi R, Colombo N. Neoadjuvant chemotherapy in cervical cancer: an update. *Expert Review of Anticancer Therapy*. 2015;15(10):1171-1181. <https://doi.org/10.1586/14737140.2015.1079777>
10. Kumar L, Harish P, Malik PS, Khurana S. Chemotherapy and targeted therapy in the management of cervical cancer. *Current Problems in Cancer*. 2018;42(2):120-128. <https://doi.org/10.1016/j.currprobcancer.2018.01.016>
11. Pectasides D, Kamposioras K, Papaxoinis G, Pectasides E. Chemotherapy for recurrent cervical cancer. *Cancer Treatment Reviews*. 2008 Nov;34(7):603-613. <https://doi.org/10.1016/j.ctrv.2008.05.006>
12. Hashim1 WS, Jumaa2 AH, Alsaadi 1 NT, Arian1 AG. Physiological Study Comprising the Sequelae of Magnetic Radiation on Human. *Indian Journal of Forensic Medicine & Toxicology*. 2020 04 29;14(2):421-425. <https://doi.org/10.37506/ijfimt.v14i2.2828>
13. Zhang M, et al. Identify Key Genes of Ferroptosis and reveals its relationship with immune in Gliomas of different grades: Integrative Analysis from Bioinformatics. 2024;.
14. Yurttas AG, Dasci MF. Exploring the molecular mechanism of linagliptin in osteosarcoma cell lines for anti-cancer activity. *Pathology, Research and Practice*. 2023 08;248:154640. <https://doi.org/10.1016/j.prp.2023.154640>
15. Muafaq Said A, Abdulla KN, Ahmed NH, Yasin YS. Antiproliferative Impact of Linagliptin on the Cervical Cancer Cell Line. *Asian Pacific journal of cancer prevention: APJCP*. 2024 09 01;25(9):3293-3300. <https://doi.org/10.31557/APJCP.2024.25.9.3293>
16. Chueca E, Apostolova N, Esplugues JV, García-González MA, Lanas Á, Piazuelo E. Proton Pump Inhibitors Display Antitumor Effects in Barrett's Adenocarcinoma Cells. *Frontiers in Pharmacology*. 2016;7:452. <https://doi.org/10.3389/fphar.2016.00452>
17. Fako VE, Wu X, Pflug B, Liu J, Zhang J. Repositioning proton pump inhibitors as anticancer drugs by targeting the thioesterase domain of human fatty acid synthase. *Journal of Medicinal Chemistry*. 2015 01 22;58(2):778-784. <https://doi.org/10.1021/jm501543u>
18. Lu ZN, Tian B, Guo XL. Repositioning of proton pump inhibitors in cancer therapy. *Cancer Chemotherapy and Pharmacology*. 2017 Nov;80(5):925-937. <https://doi.org/10.1007/s00280-017-3426-2>
19. Zhang B, Yang Y, Shi X, Liao W, Chen M, Cheng AS, Yan H, et al. Proton pump inhibitor pantoprazole abrogates adriamycin-resistant gastric cancer cell invasiveness via suppression of Akt/GSK- β /catenin signaling and epithelial-mesenchymal transition. *Cancer Letters*. 2015 01 28;356(2 Pt B):704-712. <https://doi.org/10.1016/j.canlet.2014.10.016>
20. Feng S, Zheng Z, Feng L, Yang L, Chen Z, Lin Y, Gao Y, Chen Y. Proton pump inhibitor pantoprazole inhibits the proliferation, self renewal and chemoresistance of gastric cancer stem cells via the EMT/ β catenin pathways. *Oncology Reports*. 2016 Dec;36(6):3207-3214. <https://doi.org/10.3892/or.2016.5154>
21. Hebert KA, Bonnen MD, Ghebre YT. Proton pump inhibitors and sensitization of cancer cells to radiation therapy. *Frontiers in Oncology*. 2022;12:937166. <https://doi.org/10.3389/fonc.2022.937166>
22. Babu D, Mudiraj A, Yadav N, Y B V K C, Panigrahi M, Prakash Babu P. Rabeprazole has efficacy per se and reduces resistance to temozolomide in glioma via EMT inhibition. *Cellular Oncology* (Dordrecht, Netherlands). 2021 08;44(4):889-905. <https://doi.org/10.1007/s13402-021-00609-w>
23. Martínez-Zaguilán R, S.R. Sennoune. Vacuolar H⁺-ATPase Signaling in Cancer. Regulation of Ca²⁺-ATPases, V-ATPases and F-ATPases. 2016;;p. 371-392.
24. Slobbe G. Anti-cancer mechanisms of the most used drugs worldwide: old drugs, new insights. 2022;.
25. Ribatti D, Tamma R, Annese T. Epithelial-Mesenchymal Transition in Cancer: A Historical Overview. *Translational Oncology*. 2020 06;13(6):100773. <https://doi.org/10.1016/j.tranon.2020.100773>
26. Antony J, Thiery GP, Huang RY. Epithelial-to-mesenchymal transition: lessons from development, insights into cancer and the potential of EMT-subtype based therapeutic intervention. *Physical Biology*. 2019 05 07;16(4):041004. <https://doi.org/10.1088/1478-3975/ab157a>
27. Hanahan D, R.A. Weinberg. Hallmarks of cancer. An organizing principle for cancer medicine. *Primer of the molecular biology of cancer*. 2nd ed. Philadelphia: Wolters Kluwer. 2015;;p. 28-57.
28. Skrzypek K, Majka M. Interplay among SNAIL Transcription Factor, MicroRNAs, Long Non-Coding RNAs, and Circular RNAs in the Regulation of Tumor Growth and Metastasis. *Cancers*. 2020 01 14;12(1):209. <https://doi.org/10.3390/cancers12010209>
29. Skrypek N, Goossens S, De Smedt E, Vandamme N, Berx G. Epithelial-to-Mesenchymal Transition: Epigenetic Reprogramming Driving Cellular Plasticity. *Trends in genetics: TIG*. 2017 Dec;33(12):943-959. <https://doi.org/10.1016/j.tig.2017.08.004>
30. Yang J, Hou Y, Zhou M, Wen S, Zhou J, Xu L, Tang X, et al. Twist induces epithelial-mesenchymal transition and cell motility in breast cancer via ITGB1-FAK/ILK signaling axis and its associated downstream network. *The International Journal of Biochemistry & Cell Biology*. 2016 02;71:62-71. <https://doi.org/10.1016/j.biocel.2015.12.004>
31. Jarad A. Diabetic wound healing enhancement by tadalafil. 2020;.
32. Li Y, Ren B, Li H, Lu T, Fu R, Wu Z. Omeprazole suppresses aggressive cancer growth and metastasis in mice through promoting Snail degradation. *Acta Pharmacologica Sinica*. 2022 07;43(7):1816-1828. <https://doi.org/10.1038/s41401-021-00787-1>
33. Bakir B, Chiarella AM, Pitarresi JR, Rustgi AK. EMT, MET, Plasticity, and Tumor Metastasis. *Trends in Cell Biology*. 2020 Oct;30(10):764-776. <https://doi.org/10.1016/j.tcb.2020.07.003>
34. Muranova LK, Shatov VM, Bukach OV, Gusev NB. Cardio-Vascular Heat Shock Protein (cvHsp, HspB7), an Unusual Representative of Small Heat Shock Protein Family. *Biochemistry. Biokhimiia*. 2021 01;86(Suppl 1):S1-S11. <https://doi.org/10.1134/S0006297921140017>
35. Nover L. Chromatin Structure, Transcription, and Pre-mRNP Processing, in Heat shock response. 2022, CRC Press;;p. 263-279.
36. Regimbeau M, Abrey J, Vautrot V, Causse S, Gobbo J, Garrido C. Heat shock proteins and exosomes in cancer theranostics. *Seminars in Cancer Biology*. 2022 Nov;86(Pt 1):46-57. <https://doi.org/10.1016/j.semcancer.2021.07.014>
37. Concannon CG, Orrenius S, Samali A. Hsp27

- inhibits cytochrome c-mediated caspase activation by sequestering both pro-caspase-3 and cytochrome c. *Gene Expression*. 2001;9(4-5):195-201. <https://doi.org/10.3727/000000001783992605>
38. Le TK, Cherif C, Omabe K, Paris C, Lannes F, Audebert S, Baudalet E, et al. DDX5 mRNA-targeting antisense oligonucleotide as a new promising therapeutic in combating castration-resistant prostate cancer. *Molecular Therapy: The Journal of the American Society of Gene Therapy*. 2023 02 01;31(2):471-486. <https://doi.org/10.1016/j.ymthe.2022.08.005>
 39. Shiota M, Itsumi M, Takeuchi A, Imada K, Yokomizo A, Kuruma H, Inokuchi J, et al. Crosstalk between epithelial-mesenchymal transition and castration resistance mediated by Twist1/AR signaling in prostate cancer. *Endocrine-Related Cancer*. 2015 Dec;22(6):889-900. <https://doi.org/10.1530/ERC-15-0225>
 40. Lettini G, Lepore S, Crispo F, Sisinni L, Esposito F, Landriscina M. Heat shock proteins in cancer stem cell maintenance: A potential therapeutic target?. *Histology and Histopathology*. 2020 01;35(1):25-37. <https://doi.org/10.14670/HH-18-153>
 41. Singh MK, Sharma B, Tiwari PK. The small heat shock protein Hsp27: Present understanding and future prospects. *Journal of Thermal Biology*. 2017 Oct;69:149-154. <https://doi.org/10.1016/j.jtherbio.2017.06.004>
 42. Venugopal A, Sundaramoorthy K, Vellingiri B. Therapeutic potential of Hsp27 in neurological diseases. *Egyptian Journal of Medical Human Genetics*. 2019 Nov 05;20(1):21. <https://doi.org/10.1186/s43042-019-0023-4>
 43. Choi S, Kam H, Kim K, Park SI, Lee Y. Targeting Heat Shock Protein 27 in Cancer: A Druggable Target for Cancer Treatment?. *Cancers*. 2019 08 16;11(8):1195. <https://doi.org/10.3390/cancers11081195>
 44. Yang C, Wang H, Zhu D, Hong CS, Dmitriev P, Zhang C, Li Y, et al. Mutant glucocerebrosidase in Gaucher disease recruits Hsp27 to the Hsp90 chaperone complex for proteasomal degradation. *Proceedings of the National Academy of Sciences of the United States of America*. 2015 01 27;112(4):1137-1142. <https://doi.org/10.1073/pnas.1424288112>
 45. Nahomi RB, DiMauro MA, Wang B, Nagaraj RH. Identification of peptides in human Hsp20 and Hsp27 that possess molecular chaperone and anti-apoptotic activities. *The Biochemical Journal*. 2015 01 01;465(1):115-125. <https://doi.org/10.1042/BJ20140837>
 46. Concannon CG, Gorman AM, Samali A. On the role of Hsp27 in regulating apoptosis. *Apoptosis: An International Journal on Programmed Cell Death*. 2003 01;8(1):61-70. <https://doi.org/10.1023/a:1021601103096>
 47. Spigel DR, Shipley DL, Waterhouse DM, Jones SF, Ward PJ, Shih KC, Hemphill B, et al. A Randomized, Double-Blinded, Phase II Trial of Carboplatin and Pemetrexed with or without Apatorsen (OGX-427) in Patients with Previously Untreated Stage IV Non-Squamous-Non-Small-Cell Lung Cancer: The SPRUCE Trial. *The Oncologist*. 2019 Dec;24(12):e1409-e1416. <https://doi.org/10.1634/theoncologist.2018-0518>
 48. Salehi B, Fokou PVT, Yamthe LRT, Tali BT, Adetunji CO, Rahavian A, Mudau FN, et al. Phytochemicals in Prostate Cancer: From Bioactive Molecules to Upcoming Therapeutic Agents. *Nutrients*. 2019 06 29;11(7):1483. <https://doi.org/10.3390/nu11071483>
 49. Phillips PA, Dudeja V, McCarroll JA, Borja-Cacho D, Dawra RK, Grizzle WE, Vickers SM, Saluja AK. Triptolide induces pancreatic cancer cell death via inhibition of heat shock protein 70. *Cancer Research*. 2007 Oct 01;67(19):9407-9416. <https://doi.org/10.1158/0008-5472.CAN-07-1077>
 50. Karademir D, Özgür A. Small molecule heat shock protein 27 inhibitor J2 decreases ovarian cancer cell proliferation via induction of apoptotic pathways. *Medical Oncology (Northwood, London, England)*. 2023 07 26;40(9):250. <https://doi.org/10.1007/s12032-023-02126-2>
 51. Asgharzadeh F, Moradi-Marjaneh R, Marjaneh MM. The Role of Heat Shock Protein 40 in Carcinogenesis and Biology of Colorectal Cancer. *Current Pharmaceutical Design*. 2022;28(18):1457-1465. <https://doi.org/10.2174/1381612828666220513124603>
 52. Sun B, Li G, Yu Q, Liu D, Tang X. HSP60 in cancer: a promising biomarker for diagnosis and a potentially useful target for treatment. *Journal of Drug Targeting*. 2022 01;30(1):31-45. <https://doi.org/10.1080/1061186X.2021.1920025>
 53. Kang M, Jeong S, An J, Park S, Nam S, Kwon KA, Sahoo D, Ghosh P, Kim JH. Clinicopathologic Significance of Heat Shock Protein 60 as a Survival Predictor in Colorectal Cancer. *Cancers*. 2023 08 11;15(16):4052. <https://doi.org/10.3390/cancers15164052>
 54. Lianos GD, Alexiou GA, Mangano A, Mangano A, Rausei S, Boni L, Dionigi G, Roukos DH. The role of heat shock proteins in cancer. *Cancer Letters*. 2015 05 01;360(2):114-118. <https://doi.org/10.1016/j.canlet.2015.02.026>
 55. Cho SY, Kang S, Kim DS, Na HJ, Kim YJ, Choi YD, Cho NH. HSP27, ALDH6A1 and Prohibitin Act as a Trio-biomarker to Predict Survival in Late Metastatic Prostate Cancer. *Anticancer Research*. 2018 Nov;38(11):6551-6560. <https://doi.org/10.21873/anticancer.13021>
 56. Kumar S, O'Malley J, Chaudhary AK, Inigo JR, Yadav N, Kumar R, Chandra D. Hsp60 and IL-8 axis promotes apoptosis resistance in cancer. *British Journal of Cancer*. 2019 Nov;121(11):934-943. <https://doi.org/10.1038/s41416-019-0617-0>
 57. Meng Q, Li BX, Xiao X. Toward Developing Chemical Modulators of Hsp60 as Potential Therapeutics. *Frontiers in Molecular Biosciences*. 2018;5:35. <https://doi.org/10.3389/fmolb.2018.00035>
 58. Tang Y, Zhou Y, Fan S, Wen Q. The multiple roles and therapeutic potential of HSP60 in cancer. *Biochemical Pharmacology*. 2022 07;201:115096. <https://doi.org/10.1016/j.bcp.2022.115096>
 59. Jumaa AH, Al Uboody WSH, Hady AM. Esomeprazole and amygdalin combination cytotoxic effect on human cervical cancer cell line (Hela cancer cell line). *Journal of Pharmaceutical Sciences and Research*. 2018;10(9):p. 2236-2241.
 60. Jumaa AH, Jarad AS, Al Uboody WSH. The effect of esomeprazole on cell line human cervical cancer. *Medico-Legal Update*. 2020;20(1).
 61. Yasin YS, Jumaa AH, Jabbar S, Abdulkareem AH. Effect of Laetrile Vinblastine Combination on the Proliferation of the Hela Cancer Cell Line. *Asian Pacific journal of cancer prevention: APJCP*. 2023 Dec 01;24(12):4329-4337. <https://doi.org/10.31557/APJCP.2023.24.12.4329>
 62. Al-Samarray YSY, et al. The cytotoxic effect of ethanolic extract of *Cnicus benedictus* L. flowers on the murine mammary adenocarcinoma cancer cell line AMN-3. *ResearchGate*. 2020;.
 63. Jumaa AH, Abdulkareem AH, Yasin YS. The Cytotoxic Effect of Ciprofloxacin Laetrile Combination on Esophageal Cancer Cell Line. *Asian Pacific journal of cancer prevention: APJCP*. 2024 04 01;25(4):1433-1440. <https://doi.org/10.31557/APJCP.2024.25.4.1433>
 64. Rutledge SJAP. What HeLa Cells Are You Using? . 2023;.
 65. Sharma AK, et al. Animal cell culture, in *Clinical*

- Biochemistry and Drug Development. 2020, Apple Academic Press;p. 7-31..
66. Uysal O, Semerci Sevimli T, Sevimli M, Güneş S, Eker Sarıboyacı A. Cell and Tissue Culture: The Base of Biotechnology. Omics Technologies And Bio-Engineering: Towards Improving Quality Of Life, Vol 1: Emerging Fields, Animal And Medical Biotechnologies. 2018;. <https://doi.org/10.1016/b978-0-12-804659-3.00017-8>
 67. Zhang Y, Qi D, Gao Y, Liang C, Zhang Y, Ma Z, Liu Y, et al. History of uses, phytochemistry, pharmacological activities, quality control and toxicity of the root of *Stephania tetrandra* S. Moore: A review. *Journal of Ethnopharmacology*. 2020 Oct 05;260:112995. <https://doi.org/10.1016/j.jep.2020.112995>
 68. Bor T, et al. Antimicrobials from herbs, spices, and plants, in Fruits, vegetables, and herbs. 2016, Elsevier;; p. 551-578.
 69. Bezerra JN, Gomez MCV, Rolón M, Coronel C, Almeida-Bezerra JW, Fidelis KR, Menezes SA, et al. Chemical composition, evaluation of antiparasitary and cytotoxic activity of the essential oil of *Psidium brownianum* MART ex. DC.. 2022;39. <https://doi.org/10.1016/j.bcab.2021.102247>
 70. Salentin S, Schreiber S, Haupt VJ, Adasme MF, Schroeder M. PLIP: fully automated protein-ligand interaction profiler. *Nucleic Acids Research*. 2015 07 01;43(W1):W443-447. <https://doi.org/10.1093/nar/gkv315>
 71. Chen G, Seukep AJ, Guo M. Recent Advances in Molecular Docking for the Research and Discovery of Potential Marine Drugs. *Marine Drugs*. 2020 Oct 30;18(11):545. <https://doi.org/10.3390/md18110545>
 72. Meyer CT, Wooten DJ, Lopez CF, Quaranta V. Charting the Fragmented Landscape of Drug Synergy. *Trends in Pharmacological Sciences*. 2020 04;41(4):266-280. <https://doi.org/10.1016/j.tips.2020.01.011>
 73. Chou T. The combination index (CI < 1) as the definition of synergism and of synergy claims. *Synergy*. 2018 Dec 01;7:49-50. <https://doi.org/10.1016/j.synres.2018.04.001>
 74. Cary, N.J.S.I.I.U. Statistical analysis system, User's guide. Statistical. Version 9. 2012.
 75. GuoLT, et al. Qsar Aided Design of Potent Ret Inhibitors Using Molecular Docking, Molecular Dynamics Simulation and Binding Free Energy Calculation. *Molecular Dynamics Simulation and Binding Free Energy Calculation*. 2024.
 76. Miura A, Narita Y, Sugawara T, Shimizu H, Itoh H. Mizoribine Promotes Molecular Chaperone HSP60/HSP10 Complex Formation. *International Journal of Molecular Sciences*. 2024 06 12;25(12):6452. <https://doi.org/10.3390/ijms25126452>
 77. Mahdi HM, Wade SA . Interaction Effect of Methotrexate and Aspirin on MCF7 cell line Proliferation: In vitro Study. *Journal of Advanced Veterinary Research*. 2023;13(9):1767-71.
 78. Li Y, et al. Repositioning of hypoglycemic drug linagliptin for cancer treatment. 2020;11:496241.
 79. Li Y, Li Y, Li D, Li K, Quan Z, Wang Z, Sun Z. Repositioning of Hypoglycemic Drug Linagliptin for Cancer Treatment. *Frontiers in Pharmacology*. 2020;11:187. <https://doi.org/10.3389/fphar.2020.00187>
 80. Lucena-Araujo AR, Oliveira FM, Leite-Cueva SD, Santos GA, Falcao RP, Rego EM. High expression of AURKA and AURKB is associated with unfavorable cytogenetic abnormalities and high white blood cell count in patients with acute myeloid leukemia. *Leukemia Research*. 2011 02;35(2):260-264. <https://doi.org/10.1016/j.leukres.2010.07.034>
 81. Xu Q, Jia X, Wu Q, Shi L, Ma Z, Ba N, Zhao H, Xia X, Zhang Z. Esomeprazole affects the proliferation, metastasis, apoptosis and chemosensitivity of gastric cancer cells by regulating lncRNA/circRNA miRNA mRNA ceRNA networks. *Oncology Letters*. 2020 Dec 01;20(6):1-1. <https://doi.org/10.3892/ol.2020.12193>
 82. Lee J, Hong J, Shin H, Ryu C, Park S, Jeong SH. Overexpression of V-ATPase B2 attenuates lung injury/fibrosis by stabilizing lysosomal membrane permeabilization and increasing collagen degradation. *Experimental & Molecular Medicine*. 2022 05;54(5):662-672. <https://doi.org/10.1038/s12276-022-00776-2>
 83. Eriksson I, Öllinger K, Appelqvist H. Analysis of Lysosomal pH by Flow Cytometry Using FITC-Dextran Loaded Cells. *Methods in Molecular Biology* (Clifton, N.J.). 2017;1594:179-189. https://doi.org/10.1007/978-1-4939-6934-0_11



This work is licensed under a Creative Commons Attribution-Non Commercial 4.0 International License.